

Majorana chiral spin liquid in Mott insulating cuprates

Jaime Merino

*Departamento de Física Teórica de la Materia Condensada,
Condensed Matter Physics Center (IFIMAC) and Instituto Nicolás Cabrera,
Universidad Autónoma de Madrid, Madrid 28049, Spain*

Arnaud Ralko

Institut Néel, Université Grenoble Alpes et CNRS UPR2940, Grenoble 38042, France

(Dated: January 3, 2022)

The large thermal Hall conductivity recently detected in Mott insulating cuprates has been attributed to chiral neutral spin excitations. A quantum spin liquid with Majorana excitations, Chern number ± 4 and large thermal Hall conductivity is found to be an excited state of a frustrated Heisenberg model on the square lattice. Using a Majorana mean-field theory and exact diagonalizations, we explore two possible routes to achieve this chiral quantum spin liquid, an orbital effect of an applied magnetic field and spin orbit couplings as present in cuprates. In particular, we show how only the orbital magnetic field allows this topological phase to be the ground state, while it remains an excited state of the Majorana mean field under the Dzyaloshinskii-Moriya terms. We interpret the large thermal Hall effect observed in Mott cuprates from their close proximity to a transition to a Majorana chiral quantum spin liquid which can be induced by an external magnetic field.

Introduction. The pseudogap phase of the cuprates continues to provide unexpected behavior. Thermal Hall experiments have recently found a surprisingly large thermal Hall conductivity¹. As doping is reduced below the critical doping $\delta < \delta^*$, a negative thermal Hall conductivity signal is observed, which becomes the largest when reaching the Mott insulator $\delta \approx 0$. The large absolute values and T -dependence of the thermal Hall conductivity in the undoped cuprate, La_2CuO_4 , is very similar to observations in several spin liquid frustrated materials such as volborthite² or $\alpha\text{-RuCl}_3$ ³. The half-quantization thermal Hall effect⁴ observed in $\alpha\text{-RuCl}_3$ is interpreted in terms of Majorana edge modes arising in the Kitaev spin liquid under an external magnetic field. It is then an open question whether the Mott and pseudogap phases of cuprates host unconventional neutral chiral excitations which can lead to the observed large thermal Hall effect.

Phonons have been identified as the main heat carriers in the thermal Hall effect observed in the pseudogap⁵ and Mott insulating phases⁶ of cuprates. The large values of the thermal Hall conductivity indicates that phonons have non-zero chirality whose origin is yet to be explained. Since magnetic impurity effects and magnons have been discarded, a possible scenario is that the paramagnetic phase of cuprates is a quantum spin liquid whose chirality is imprinted on the phonons through the spin-phonon coupling. An intriguing theoretical possibility would be a chiral quantum spin liquid on the square lattice with Majorana fermions as elementary excitations, as in the Kitaev quantum spin liquid in the honeycomb lattice, relevant to $\alpha\text{-RuCl}_3$. Other related but different chiral quantum spin liquids with either bosonic^{7,8} or fermionic spinons⁹ have been proposed in undoped cuprates. The d -density wave¹⁰ has non-fractional electron constituents for $\delta \neq 0$ though.

Here, we show how a chiral spin liquid state with Ma-

ajorana excitations is a good candidate for explaining the thermal Hall effect in Mott insulating cuprates. Using a Majorana representation of the J_1 - J_2 Heisenberg model on the square lattice, we find that a chiral spin liquid state breaking time-reversal symmetry with Majorana excitations emerges spontaneously. Such state which we denote as Majorana π -QSL has a large associated Chern number $\nu = \pm 4$, leading to absolute values of the thermal Hall conductivity of the order $\sim k_B^2/\hbar$ as experimentally observed. However, this chiral spin liquid state is only an excited state of the system: the well known Néel, collinear and/or non-chiral disordered states being favored for different ranges of magnetic frustration. Extending the Heisenberg model to account for the presence of an external magnetic field through the orbital effect and/or for a Dzyaloshinskii-Moriya (DM) spin orbit coupling, we explore whether the π -QSL becomes the absolute ground state of the system or not. Considering several compatible choices of DM vectors, we show how the π -QSL is lowered in energy by the DM but always remains an excited state of the system. Only the orbital magnetic field is able to turn the π -QSL into the absolute ground state, consistent with observations where the magnetic field is essential to externally trigger the transition. Hence, the combined effect of the DM and the magnetic field orbital term can drive the relevant model for Mott insulating cuprates into the Majorana π -QSL phase which displays the large thermal Hall effect experimentally observed.

Model and methods. The simplest relevant model to describe the magnetic properties of undoped cuprates is the J_1 - J_2 $S = 1/2$ Heisenberg model on the square lattice:

$$H_{\text{H}} = J_1 \sum_{\langle ij \rangle} \mathbf{S}_i \cdot \mathbf{S}_j + J_2 \sum_{\langle\langle ij \rangle\rangle} \mathbf{S}_i \cdot \mathbf{S}_j \quad (1)$$

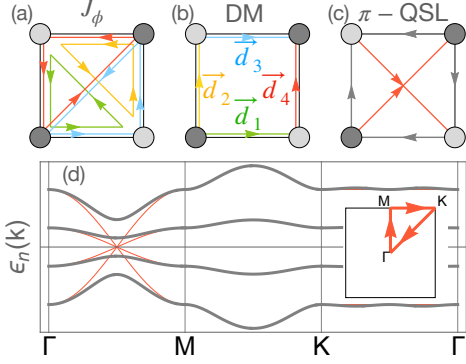


FIG. 1: Majorana chiral quantum spin liquid state in the J_1 - J_2 Heisenberg model on a square lattice. (a) and (b) Bond conventions used for the orbital magnetic field term and the Dzyaloshinskii-Moriya interactions. (c) The bond patterns of the MMFT lowest energy QSL, the π -QSL. The arrows indicate that the bond average is positive (negative) in the same (opposite) direction of a bond between two sites. (d) Excitation spectra of the gapless π -QSL for $J_2 = 0$ (red) and of the gapped π -QSL arising for $J_2 \neq 0$ ($J_2 = J_1/2$ in this plot). The Brillouin zone with high symmetry points is displayed as an inset.

where the first sum runs over nearest-neighbor sites and the second over next nearest neighbors.

Electrons can couple to an external magnetic field B through their orbital motion. A strong coupling expansion of the Hubbard model to $\mathcal{O}(t^3/U^2)$ leads to the additional chiral term¹¹:

$$H_\phi = J_\phi \sum_{\Delta} T_{ijk} = J_\phi \sum_{\Delta} \mathbf{S}_i \cdot (\mathbf{S}_j \times \mathbf{S}_k), \quad (2)$$

where Δ denotes a triangle lying in the square plaquettes of area A with vertices ijk taken in an anticlockwise direction (see Fig.1(b)). The three-spin-exchange coupling is $J_\phi = -\frac{24t_2t_1^2}{U^2} \sin(2\pi\phi/\phi_0)$, with $\phi = BA/2$ and $\phi_0 = hc/e$ the flux quantum.

A second important ingredient is the spin-orbit coupling effect through the Dzyaloshinskii-Moriya (DM) interaction¹²⁻¹⁴ defined as:

$$H_{\text{DM}} = \sum_{\langle i,j \rangle} \mathbf{D}_{ij} \cdot (\mathbf{S}_i \times \mathbf{S}_j) \quad (3)$$

where \mathbf{D}_{ij} are DM vectors. The compatible vectors \mathbf{D}_{ij} are generically defined by 4 unit vectors \vec{d}_i with $i = 1, 2, 3, 4$ pointing in the different bond directions of a 4-site unit cell, as given in Fig.1(b). We consider in this work several cases to explore the possibility of spin orbit coupling to lead to a chiral liquid state: SO compatible with cuprates like YBCO, LSCO-LTO, LSCO-LTT as defined in [7], or SO corresponding to *Rashba-like* and *Dresselhaus-like* couplings [15] (see Supplemental Material [26] for details).

We introduce the Majorana representation of the spins consisting on four Majorana fermion operators c, b^x, b^y, b^z

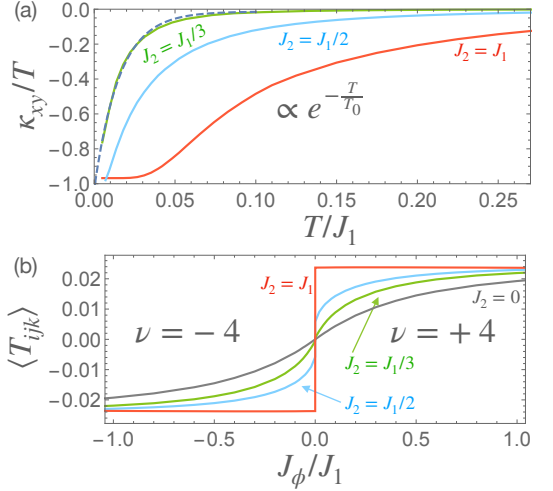


FIG. 2: (a) Thermal Hall conductivity of the π -QSL on the square lattice. The T -dependence of κ_{xy}/T in units of k_B^2/\hbar is shown for different J_2/J_1 . The π -QSL leads to large absolute values of $\kappa_{xy}/T \sim -k_B^2/\hbar$ as $T \rightarrow 0$ and an intermediate T -dependence $\kappa_{xy}/T \propto e^{-T/T_0}$ consistent with observations in undoped cuprates. From such exponential fit to the $J_2 = J_1/3$ theoretical results we obtain a $T_0 \approx 18$ K (assuming $J_1 \sim 0.1$ eV), very close to experimental values, $T_0^{\text{expt}} \approx 16 - 18$ K for La_2CuO_4 and $\text{Sr}_2\text{CuO}_2\text{Cl}_2$. (b) Dependence of the chirality of the π -QSL state with J_ϕ obtained from MMFT. Dependence of the Chern number of the π -QSL state with J_ϕ for all J_2 .

per site as used by Kitaev¹⁷ to exactly solve his spin model (see the Supplemental Material [26]). In this representation, the spin operators are $S_i^\alpha = \frac{i}{2} b_i^\alpha c_i$, where $\alpha = x, y, z$. A three-channel mean-field decoupling of the interaction terms $S_i^\alpha S_j^\beta$ in the Hamiltonian yields to

$$\begin{aligned} & + \frac{1}{4} \left[\langle b_i^\alpha c_i \rangle b_j^\beta c_j + \langle b_j^\beta c_j \rangle b_i^\alpha c_i - \langle b_i^\alpha c_i \rangle \langle b_j^\beta c_j \rangle \right] \\ & - \frac{1}{4} \left[\langle b_i^\alpha b_j^\beta \rangle c_i c_j + \langle c_i c_j \rangle b_i^\alpha b_j^\beta - \langle b_i^\alpha b_j^\beta \rangle \langle c_i c_j \rangle \right] \\ & + \frac{1}{4} \left[\langle b_i^\alpha c_j \rangle b_j^\beta c_i + \langle b_j^\beta c_i \rangle b_i^\alpha c_j - \langle b_i^\alpha c_j \rangle \langle b_j^\beta c_i \rangle \right] \end{aligned} \quad (4)$$

where the first three terms are associated with magnetic orders while the next three with spin liquid formation.

With such decoupling, our Majorana mean-field theory¹⁸ (MMFT) allows to analyze on equal footing quantum spin liquids (QSL) ($\langle \mathbf{S}_i \rangle = 0$) as well as magnetically ordered states. To do so, as done in [18], we solve numerically the set of self consistent equations, together with a physical constraint connected to the number of particles per site that our theory has to fulfill.

Chiral QSL with Majorana excitations. The J_1 - J_2 Heisenberg model on the square lattice sustains a chiral quantum spin liquid state with Majorana fermion excitations (see Supplemental Material [26]). Among the possible QSL ansätze, the π -flux QSL ansatz or π -QSL from now on, shown Fig.1(c) has the lowest energy in a finite range of J_2 , consistent with Lieb's theorem¹⁹.

The eight corresponding Majorana bands – there are two sites per unit-cell²⁰, labelled A and B – are given by $\pm 3\gamma(\mathbf{k}), \pm\gamma(\mathbf{k})$ (triply degenerate) with

$$\gamma(\mathbf{k}) = \frac{J_1}{2} \sqrt{c_1^2 (\sin^2 k_x + \cos^2 k_y) + (2\frac{J_2}{J_1} c_2 \cos k_x \sin k_y)^2}$$

where we have defined $c_1 = \langle c_{i_A} i c_{j_B} \rangle = \langle b_{i_A}^\alpha i b_{j_B}^\alpha \rangle$ and $c_2 = \langle c_{i_A} i c_{j_A} \rangle = \langle b_{i_A}^\alpha i b_{j_A}^\alpha \rangle$. For $J_2 = 0$, all these bands touch at the two Dirac points $(0, \pm\pi/2)$ in the Brillouin zone as shown in Fig.1(d), the π -QSL is gapless in this case. Moreover, it minimizes the total energy with $E = -0.3442J_1$ much lower than the 0-flux QSL ansatz with $E = -0.2462J_1$. The $\pm\pi$ Berry phases at the Dirac cones can lead to non-trivial topology if the gap opens in a non-trivial manner. Indeed, this occurs when turning on a $J_2 \neq 0$, as shown in Fig.1(d). The gap opening lowers slightly the energy from $E = -0.3442J_1$ ($|c_1| = 0.4790$) for $J_2 = 0$ to $E = -0.3443J_1$ ($|c_1| = 0.4777$, $|c_2| = 0.0516$) for $J_2 = 0.5$ and to $E = -0.3726J_1$ ($|c_1| = 0.4189$, $|c_2| = 0.2700$) for $J_2 = J_1$. Moreover, a direct calculation of the topological invariant Chern number ν on the occupied Majorana bands¹⁸ (with negative energy) shows that this state is a gapped topological π -QSL with $\nu = \pm 4$.

In Fig. 2(a) we show the thermal Hall conductivity of the π -QSL obtained from the expression:²¹

$$\frac{\kappa_{xy}}{T} = \frac{k_B^2}{\hbar} \frac{1}{8(k_B T)^3} \int d\epsilon \frac{(\epsilon - \mu)^2}{\cosh^2[\beta(\epsilon - \mu)/2]} \sigma_{xy}(\epsilon), \quad (5)$$

where $\sigma_{xy}(\epsilon) = \sum_{n\mathbf{k}} \Omega_n^z(\mathbf{k}) \theta(\epsilon - \epsilon_n(\mathbf{k}))$. Note that the r.h.s. of Eq. 5 is half of the standard expression used for fermionic spinons since in our MMFT approach, thermal energy is transported by the Majoranas. In the limit $T \rightarrow 0$, we find $\kappa_{xy}/T \rightarrow -(k_B^2/\hbar)$ since each of the occupied bands carries a Chern number of -1 . The overall absolute values and T -dependence of κ_{xy}/T are consistent with observations (see Supplemental Material [26]). As temperature is raised and thermal excitations of the Majorana fermions occur, there is a cancellation between the Chern numbers of the bands above and below zero energy and $\kappa_{xy}/T \rightarrow 0$.

The gapped π -QSL found in the J_1 - J_2 Heisenberg model for $J_2 \neq 0$ is doubly-degenerate since there are two possible senses of the bond amplitudes or chiralities, $\langle T_{ijk} \rangle \neq 0$, with the same energy. Hence, the Chern number of the π -QSL can have two values, $\nu = \pm 4$, depending on the sign of the chirality as shown in Fig.2(b). It may seem that spontaneous symmetry breaking can occur since any infinitesimal $J_\phi \rightarrow 0^\pm$ selects either the $\nu = 4$ or the $\nu = -4$ π -QSL solution. However, our MMFT stability analysis below reveals that the π -QSL is only an excitation of the pure J_1 - J_2 Heisenberg model. Under a finite J_ϕ , the π -QSL with the favorable sign of the chirality for the orientation of the applied B , becomes the ground state of the system. This is consistent with experiments on the cuprates which find no thermal Hall effect when no magnetic field is applied implying

no spontaneous time-reversal symmetry breaking ground state.

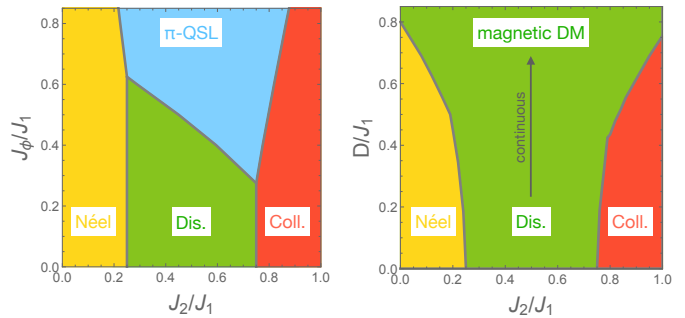


FIG. 3: Phase diagrams of the J_ϕ and D models obtained from Majorana mean field theory for cluster of $2 \times 32 \times 32$ sites. Left: orbital magnetic field, J_ϕ , model. The intermediate phase (blue region) is the π -flux QSL with topological Chern number of $\nu = \pm 4$. Right: Dzyaloshinskii-Moriya, D model. For any choice of the DM couplings, a spin disordered phase is stabilized and a continuous transition to the respective classical magnetic state is observed (arrow).

Orbital magnetic field and spin-orbit coupling effects. We have performed fully self-consistent MMFT calculations on the J_1 - J_2 - J_ϕ model (see Supplemental Material [26]). The resulting phase diagram shown in Fig.3 (a) displays Néel, stripe and spin disordered phases. For $J_\phi = 0$ we qualitatively recover the phase diagram of the J_1 - J_2 Heisenberg model on the square lattice. Subject of an intense research activity since the discovery of cuprate superconductivity, recent state-of-the-art numerical works²²⁻²⁵ find a gapless quantum spin liquid and a valence bond solid around $J_2/J_1 \sim 0.5$. Our MMFT is partially consistent with this since it predicts a spin disor-

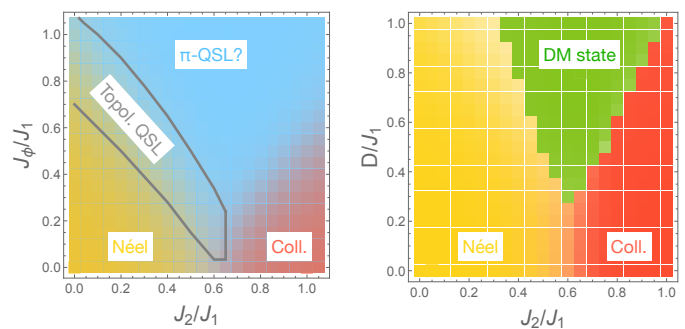


FIG. 4: Phase diagrams of the J_ϕ and D models (illustrated for YBCO) obtained from ED calculations on a 4×4 cluster based on a quantum fidelity analysis. The more intense the color, the closest to 1 the fidelity. Three reference states are used, (i) the pure Néel at point $J_2 = J_\phi = D = 0$ (yellow), (ii) the collinear state $J_2 = 1, J_\phi = D = 0$ (red) and (iii) the intermediate phase (blue) at $J_2 = 0.6, J_\phi = D = 1.0$. Left: orbital magnetic field, J_ϕ model presenting an intermediate topological QSL. Right: Dzyaloshinskii-Moriya, D model and its first order transition to a DM state driven by D .

dered valence bond crystal (VBC) phase sandwiched between the magnetically ordered Néel and collinear phases. Note that, at the mean field level, all VBCs like the columnar or the staggered phases, as well as possible resonating placquette phases²⁰ are degenerate all consisting of disconnected singlets. On the other hand, under sufficient strong J_ϕ , the MMFT finds that the π -QSL becomes the ground state in a broad region of the J_2 - J_ϕ phase diagram. Although nonphysical large J_ϕ values are needed, it is well known that mean-field theory overestimates broken symmetry states. Indeed, we show below how quantum fluctuation effects strongly suppress the critical J_ϕ at which the π -QSL emerges in the phase diagram.

We now analyze the effect of the DM interaction parameterised by the \mathbf{D} vectors (see Supplemental Material [26]). The DM is also found to favor the gapped π -QSL (with Chern number $\nu = \pm 4$) but *a contrario* to the orbital effect, it is never the absolute ground state of the J_1 - J_2 - D model. We have considered all possible MMFT self-consistent solutions analyzing in detail the competition between the π -QSL phase, the Néel and collinear magnetically ordered states and spin disordered states²⁰ for five different DM vector choices [16]. We have found that the disordered states are always the ground state and that the effect of DM is to continuously deform both the GS and the QSL to eventually reach, when D dominates, a magnetic order compatible with the considered \mathbf{D}_{ij} . The typical resulting phase diagram is shown in Fig. 3(b) for YBCO. Interestingly, this phase diagram is qualitatively similar to the phase diagram of the J_1 - J_2 - J_ϕ model discussed previously. Our MMFT results suggest that even for very large DM, $D > 0.5J_1$, not present in the cuprates ($D < 0.1J_1$), the π -QSL phase with an associated large thermal Hall effect is not the absolute ground state but still a robust and close excited state. Nevertheless, it can still play an important role in effectively bringing the system closer to the π -QSL phase. Thus, from our MMFT analysis we expect that, in the presence of the DM, the large thermal Hall effect could occur at a smaller J_ϕ than for $D = 0$.

Beyond Majorana mean-field theory. An important question is whether the π -QSL can occur beyond the MMFT approach. In Fig. 4 we show the quantum fidelity $|\langle \psi_{\text{ref}} | \psi_0 \rangle|$ where $|\psi_0\rangle$ is the ground state for a given set of parameters and $|\psi_{\text{ref}}\rangle$ is a reference state at known limiting values of the parameters (see caption of Fig. 4 for more details). For $J_\phi = D = 0$, we identify the Néel and collinear phases as well as a possible disordered phase around $J_2 \sim 0.5$ – 0.7 . We also find that the phases shown in Fig. 4 arising between the Néel and collinear phase under J_ϕ or under D are quite different. ED calculations of the spin structure factor (see Supplemental Material [26]) and spin chirality $\langle T_{ijk} \rangle$ suggest that, while the intermediate phase is spin disordered (blue region) and chiral, $\langle T_{ijk} \rangle \neq 0$, in the J_ϕ model, in the D -model it is non-chiral, $\langle T_{ijk} \rangle = 0$ and possibly also spin disordered as discussed below (green region). It however has to connect with the pure D limit at which magnetic order in-

duced by D eventually sets in. Based on the consistent comparison of the ED and the MMFT phase diagrams of Fig. 3, we associate the (blue) spin disordered phase region with the MMFT π -QSL and the (green) magnetic DM with MMFT DM magnetically ordered phase.

Within the intermediate spin disordered phase of the J_ϕ -model, close to the Néel phase, we find a topological QSL. This QSL is chiral characterized by a non-zero Chern number, $\nu = 1$, associated with a two-fold degenerate ground state well separated from a continuum of excited states, as reported previously.²⁷ Interestingly this phase survives down to very low J_ϕ for $J_2 \sim 0.6$ as shown in Fig. 4. In the D -model, the evidence for a distinct and possibly spin disordered phase is corroborated by calculations combining the quantum fidelity, the gap and the spin structure factor. Indeed, in contrast to the orbital magnetic field case, the spin phase induced by D is clearly delimited by a gap closing associated with level crossings (see Supplemental Material [26]) suggesting, to the best of our knowledge, a novel intermediate phase induced by spin-orbit coupling. We let the analysis of this phase as a future work.

The MMFT could be used to unveil the nature of the chiral QSLs found in other numerical studies of the Heisenberg model on the triangular lattice with four-spin terms²⁸ and with three-spin orbital magnetic field terms³⁵ and on spin models of Kagomé Mott insulators.^{29–32}

Connection with cuprate materials. In cuprates³³ $t_1 \sim 0.45$ eV, $U \sim 8$ eV, $J_1 \sim 0.1$ eV, and $t_2 \sim 0.35t_1$ (YBCO), $t_2 \sim 0.15t_1$ (LSCO) so that $J_2/J_1 \sim 0.12$ (YBCO), $J_2/J_1 \sim 0.023$ (LSCO). Since DM is only of a few meV, $D/J \lesssim 0.1$, we would predict that the system under no magnetic field is in the Néel phase as indeed is observed in undoped cuprates. If a magnetic field of $B \sim 10$ T is applied to the system, the flux term, $J_\phi/J_1 \sim 10^{-4} - 10^{-3}$ would be tiny. Based on the phase diagrams obtained here, in such parameter range appropriate for cuprate materials, $J_2/J_1 \sim 0.1$ and $J_\phi \rightarrow 0$, the system would be immersed in the Néel phase and so no thermal Hall effect would be expected based on our analysis. However, since the MMFT finds (see Supplementary Material [26]) that the π -QSL can coexist with the Néel AF, the π -QSL amplitude in the GS can still lead to a large thermal Hall effect. Such hybrid π -QSL + Néel AF state may also account for the anomaly observed around $(\pi, 0)$ in the magnon dispersion of square lattice antiferromagnets³⁴ which could result from the decay of $S = 1$ magnons into a continuum of Majorana excitations associated with the π -QSL.

Conclusions. We report a novel chiral QSL state with Majorana excitations and Chern number $\nu = \pm 4$ which occurs as an excited state of the Heisenberg model on the square lattice. The thermal Hall conductivity of such Majorana π -QSL state leads to large absolute values $|\kappa_{xy}/T| \sim (k_B^2/\hbar)$ consistent with experiments in Mott insulating cuprates. MMFT predicts that this Majorana π -QSL becomes the ground state under sufficiently large

J_ϕ consistent with a topological chiral QSL found in ED. The DM present in cuprates plays a secondary role eventually suppressing critical J_ϕ 's towards more physically realistic values. The large thermal Hall effect observed in Mott insulating cuprates can be interpreted from their proximity to a Majorana π -QSL transition which can be triggered by an external magnetic field via its orbital effect.

Acknowledgments

J. M. acknowledges financial support from (RTI2018-098452-B-I00) MINECO/FEDER, Unión Europea and the María de Maeztu Program for Units of Excellence in R&D (Grant No. CEX2018-000805-M).

- ¹ G. Grissonnanche, *et al.*, Giant thermal Hall conductivity in the pseudogap phase of cuprate superconductors, *Nature* **571**, 376 (2019).
- ² D. Watanabe, *et al.*, Emergence of nontrivial magnetic excitations in a spin-liquid state of Kagomé volborthite. *Proc. Natl. Acad. Sci. USA* **113**, 8653 (2016).
- ³ Y. Kasahara, *et al.*, Unusual thermal Hall effect in a Kitaev spin liquid candidate α -RuCl₃. *Phys. Rev. Lett.* **120**, 217205 (2018).
- ⁴ Y. Kasahara, *et al.*, Majorana quantization and half-integer thermal quantum Hall effect in a Kitaev spin liquid, *Nature (London)* **559**, 227 (2018).
- ⁵ G. Grissonnanche, *et al.*, Chiral phonons in the pseudogap phase of cuprates, *Nat. Phys.* **16** 1108 (2020).
- ⁶ M.-E. Boulanger *et al.*, Thermal Hall conductivity in the cuprate Mott insulators Nd₂CuO₄ and Sr₂CuO₂Cl₂, *Nat. Comm.* **11** 5325 (2020).
- ⁷ R. Samajdar, S. Chatterjee, S. Sachdev, and M. S. Scheurer, Thermal Hall effect in square-lattice spin liquids: A Schwinger boson mean-field study, *Phys. Rev. B* **99**, 165126 (2019).
- ⁸ R. Samajdar, M. S. Scheurer, S. Chatterjee, H. Guo, C. Xu and S. Sachdev, Enhanced thermal Hall effect in the square-lattice Néel state, *Nat. Phys.* **15**, 1290 (2019).
- ⁹ J. H. Han, J.-H. Park, and P. A. Lee, Consideration of thermal Hall effect in undoped cuprates, *Phys. Rev. B* **99**, 205157 (2019).
- ¹⁰ Z.-X. Li and D.-H. Lee, The thermal Hall conductance of two doped symmetry-breaking topological insulators, arXiv:1905.04248v3.
- ¹¹ O. I. Motrunich, Orbital magnetic field effects in spin liquid with spinon Fermi sea: possible application to κ -(ET)₂Cu₂(CN)₃, *Phys. Rev. B* **73**, 155115 (2006).
- ¹² I. Dzyaloshinskii, A thermodynamic theory of "weak" ferro-magnetism of antiferromagnetics, *J. Phys. Chem. Solids* **4**, 241 (1958).
- ¹³ T. Moriya, Anisotropic superexchange interaction and weak ferromagnetism, *Phys. Rev.* **120**, 91 (1960).
- ¹⁴ T. Moriya, New Mechanism of Anisotropic Superexchange Interaction, *Phys. Rev. Lett.* **4**, 228 (1960).
- ¹⁵ M. Kawano, Y. Onose and C. Hotta, Designing Rashba-Drusselhaus effect in magnetic insulators, *Comm. Phys.* **2**:27 (2019)
- ¹⁶ The corresponding DM vectors for the 5 cases considered in this work are given by: YBCO with $\vec{d}_1 = \vec{d}_3 = (d, 0, 0)$ and $\vec{d}_2 = \vec{d}_4 = (0, -d, 0)$, LSCO-LTO with $\vec{d}_1 = -\vec{d}_3 = (d, 0, 0)$ and $\vec{d}_2 = -\vec{d}_4 = (0, -d, 0)$, LSCO-LTT with $\vec{d}_1 = -\vec{d}_3 = (0, d, 0)$ and $\vec{d}_2 = -\vec{d}_4 = (0, d, 0)$, *Rashba* with $\vec{d}_1 = \vec{d}_3 = (0, d, 0)$ and $\vec{d}_2 = \vec{d}_4 = (-d, 0, 0)$ and *Dresselhaus* with $\vec{d}_1 = \vec{d}_3 = (0, -d, 0)$ and $\vec{d}_2 = \vec{d}_4 = (-d, 0, 0)$
- ¹⁷ A. Kitaev, Anyons in an exactly solvable model and beyond, *Ann. Phys. (Amsterdam)* **321**, 2 (2006).
- ¹⁸ A. Ralko and J. Merino, Novel Chiral Quantum Spin Liquids in Kitaev Magnets, *Phys. Rev. Lett.* **124**, 217203 (2020).
- ¹⁹ E. H. Lieb, Flux Phase of the Half-Filled Band, *Phys. Rev. Lett.* **73**, 2158 (1994).
- ²⁰ All the phases reported here are well described by a 2-site unit-cell. Note however that at large J_2 , the collinear phase can only be obtained on a 4-site unit-cell. For intermediate J_2/J_1 and $D \neq 0$, we also find a mean-field solution made of *plaquettes*. This state is rejected since it decouples all n.n.n. processes and behaves like a classical mean-field ground state not compatible with known results neither our ED calculations.
- ²¹ T. Qin, Q. Niu, and J. Shi, Energy Magnetization and the Thermal Hall Effect, *Phys. Rev. Lett.* **107**, 236601 (2011).
- ²² L. Wang and A. W. Sandvik, Critical Level Crossings and Gapless Spin Liquid in the Square-Lattice Spin-1/2 $J_1 - J_2$ Heisenberg Antiferromagnet, *Phys. Rev. Lett.* **121**, 107202 (2018).
- ²³ F. Ferrari and F. Becca, Gapless spin liquid and valence-bond solid in the $J_1 - J_2$ Heisenberg model on the square lattice: Insights from singlet and triplet excitations, *Phys. Rev. B* **102**, 014417 (2020).
- ²⁴ Wen-Yuan Liu, Shou-Shu Gong, Yu-Bin Li, Didier Poilblanc, Wei-Qiang Chen, Zheng-Cheng Gu, Gapless quantum spin liquid and global phase diagram of the spin-1/2 $J_1 - J_2$ square antiferromagnetic Heisenberg model, arXiv:2009.01821.
- ²⁵ Y. Nomura and M. Imada, Dirac-Type Nodal Spin Liquid Revealed by Refined Quantum Many-Body Solver Using Neural-Network Wave Function, Correlation Ratio, and Level Spectroscopy, *Phys. Rev. X* **11**, 031034 (2021).
- ²⁶ See Supplemental Material at <http://link.aps.org/supplemental/> for details on the Majorana mean-field theory on Heisenberg model, MMFT decoupling of three-spin J_ϕ and DM terms, ED analysis of magnetic order, and temperature dependence of thermal Hall conductivity. It includes Refs. [5,7,9,11,15,17](#).
- ²⁷ A. E. B. Nielsen, G. Sierra, and J. I. Cirac, Local models of quantum Hall states in lattices and physical implications, *Nat. Comm.* **4**, 42864 (2013).
- ²⁸ T. Cookmeyer, J. Motruk, and J. E. Moore, Four-spin terms and the origin of the chiral spin liquid in Mott insulators on the triangular lattice, *Phys. Rev. Lett.* **127**, 087201 (2021).
- ²⁹ B. Bauer, L. Cincio, B. P. Keller, M. Dolfi, G. Vidal, S. Trebst, and A. W. W. Ludwig, Chiral spin liquid and emergent anyons in a Kagomé lattice Mott insulator, *Nat. Commun.* **5**, 5137 (2014).

- ³⁰ L. Messio, B. Bernu, and C. Lhuillier, Kagomé Antiferromagnet: A Chiral Topological Spin Liquid?, Phys. Rev. Lett. **108**, 207204 (2012).
- ³¹ S.-S. Gong, W. Zhu, and D. Sheng, Emergent chiral spin liquid: Fractional quantum Hall effect in a Kagomé Heisenberg model, Sci. Rep. **4**, 6317 (2014).
- ³² Y.-C. He, D. N. Sheng, and Y. Chen, Chiral Spin Liquid in a Frustrated Anisotropic Kagome Heisenberg Model, Phys. Rev. Lett. **112**, 137202 (2014).
- ³³ E. Pavarini, I. Dasgupta, T. Saha-Dasgupta, O. Jepsen, and O. K. Andersen, Band-Structure Trend in Hole-Doped Cuprates and Correlation with T_{cmax} , Phys. Rev. Lett. **87**, 047003 (2001).
- ³⁴ B. Dalla Piazza, M. Mourigal, N. B. Christensen, G. J. Nilsen, P. Tregenna-Piggott, T. G. Perring, M. Enderle, D. F. McMorrow, D. A. Ivanov and H. M. Roennow, Fractional excitations in the square-lattice quantum antiferromagnet, Nat. Phys **11**, 62 (2015).
- ³⁵ A. Wietek and A. M. Läuchli, Phys. Rev. B **95**, 035141 (2017).

Supplementary material for Majorana chiral spin liquid in Mott insulating cuprates

Jaime Merino¹ and Arnaud Ralko²

¹*Departamento de Física Teórica de la Materia Condensada,
Condensed Matter Physics Center (IFIMAC) and Instituto Nicolás Cabrera,
Universidad Autónoma de Madrid, Madrid 28049, Spain*

²*Institut Néel, UPR2940, Université Grenoble Alpes et CNRS, Grenoble 38042, France*
(Dated: January 3, 2022)

I. MAJORANA MEAN-FIELD THEORY OF THE HEISENBERG MODEL ON SQUARE LATTICE

We first provide the details of the Majorana mean-field theory (MMFT) performed on the $J_1 - J_2$ Heisenberg model on a square lattice. We introduce a Majorana representation of the spin operators [1]:

$$S_i^\alpha = \frac{i}{2} b_i^\alpha c_i, \quad (\text{S1})$$

where $\alpha = x, y, z$. Although the Hilbert space is enlarged by the Majorana representation, the actual physical space can be recovered by imposing the set of constraints over the Majorana fermions:

$$\begin{aligned} b_i^z c_i &= b_i^y b_i^x, \\ b_i^y c_i &= b_i^x b_i^z, \\ b_i^x c_i &= b_i^z b_i^y, \end{aligned} \quad (\text{S2})$$

corresponding to a single occupancy constraint on the original fermions.

Any bilinear of spins $S_i^\alpha S_j^\beta$ can be mean-field Hartree-Fock decoupled as:

$$\begin{aligned} &+ \frac{1}{4} \left[\langle b_i^\alpha c_i \rangle b_j^\beta c_j + \langle b_j^\beta c_j \rangle b_i^\alpha c_i - \langle b_i^\alpha c_i \rangle \langle b_j^\beta c_j \rangle \right] \\ &- \frac{1}{4} \left[\langle b_i^\alpha b_j^\beta \rangle c_i c_j + \langle c_i c_j \rangle b_i^\alpha b_j^\beta - \langle b_i^\alpha b_j^\beta \rangle \langle c_i c_j \rangle \right] \\ &+ \frac{1}{4} \left[\langle b_i^\alpha c_j \rangle b_j^\beta c_i + \langle b_j^\beta c_i \rangle b_i^\alpha c_j - \langle b_i^\alpha c_j \rangle \langle b_j^\beta c_i \rangle \right] \end{aligned} \quad (\text{S3})$$

where the first three terms are associated with magnetic ordering while the rest with spin liquid formation. This decoupling is performed on the Heisenberg terms of the Hamiltonian ($\alpha = \beta$). The constraints in Eq. (S2) are enforced at the mean-field level through the set of Lagrange multipliers, $\{\lambda_i\}$. Since there is no contribution from the last three terms we neglect them in our present analysis.

In order to be able to describe collinear phases four-site unit cells are used in actual calculations. Here, we describe the implementation of the MMFT equations assuming a two-site unit cell allowing for Néel and/or π -flux QSL states. The diagonalization of the hamiltonian is performed in momentum space by first performing a Fourier transform of the Majoranas:

$$c_j^a = \sqrt{\frac{2}{N_c}} \sum_{\mathbf{k}} e^{i\mathbf{k}\mathbf{R}_j} c^a(\mathbf{k}), \quad (\text{S4})$$

where we have used here, for convenience, the notation: $c_j^0 = c_j, c_j^1 = b_j^x, c_j^2 = b_j^y, c_j^3 = b_j^z$. On the other hand, the operators in momentum space, $c^a(\mathbf{k})$, satisfy $c^a(\mathbf{k}) = c^{a\dagger}(-\mathbf{k})$ due to the property: $c_i^\alpha = c_i^{\alpha\dagger}$ which leads to standard fermionic anticommutation relations: $\{c^{a\dagger}(\mathbf{k}), c^{b\dagger}(\mathbf{k}')\} = \{c^a(\mathbf{k}), c^b(\mathbf{k}')\} = 0, \{c^a(\mathbf{k}), c^{b\dagger}(\mathbf{k}')\} = \delta_{ab}\delta(\mathbf{k} - \mathbf{k}')$. We have:

$$H^{MMF}(\mathbf{k}) = \begin{pmatrix} H_{AA}(\mathbf{k}) & H_{AB}(\mathbf{k}) \\ H_{BA}(\mathbf{k}) & H_{BB}(\mathbf{k}) \end{pmatrix}$$

where A, B are the two sublattices in which the original lattice is divided. Since the spin operators are expressed through four Majorana fermions $\{c, b^x, b^y, b^z\}$, each block, H_{ab} with $a, b = A, B$ is a 4×4 matrix.

The hamiltonian block associated with sites in the same sublattice, $a = A, B$, reads:

$$H_{aa}(\mathbf{k}) = \begin{pmatrix} H_{aa}^{00}(\mathbf{k}) & -\frac{i}{4}\lambda_{ax} & -\frac{i}{4}\lambda_{ay} & -\frac{i}{4}\lambda_{az} \\ \frac{i}{4}\lambda_{ax} & H_{aa}^{xx}(\mathbf{k}) & \frac{i}{4}\lambda_{az} & -\frac{i}{4}\lambda_{ay} \\ \frac{i}{4}\lambda_{ay} & -\frac{i}{4}\lambda_{az} & H_{aa}^{yy}(\mathbf{k}) & \frac{i}{4}\lambda_{ax} \\ \frac{i}{4}\lambda_{az} & \frac{i}{4}\lambda_{ay} & -\frac{i}{4}\lambda_{ax} & H_{aa}^{zz}(\mathbf{k}) \end{pmatrix}$$

where:

$$\begin{aligned} H_{aa}^{00}(\mathbf{k}) &= -\frac{iJ_2}{4} \sum_{\langle\langle ia, ja \rangle\rangle} \sum_{\alpha} \langle i b_{ia}^\alpha b_{ja}^\alpha \rangle e^{i\mathbf{k} \cdot \delta_{ia, ja}} \\ H_{aa}^{\alpha\alpha}(\mathbf{k}) &= -\frac{iJ_2}{4} \sum_{\langle\langle ij \rangle\rangle} \langle i c_{ia}^\alpha c_{ja}^\alpha \rangle e^{i\mathbf{k} \cdot \delta_{ia, ja}}. \end{aligned} \quad (\text{S5})$$

with: $\alpha = x, y, z$.

The hamiltonian block associated with the $A - B$ interaction reads:

$$H_{AB}(\mathbf{k}) = \begin{pmatrix} H_{AB}^{00}(\mathbf{k}) & 0 & 0 & 0 \\ 0 & H_{AB}^{xx}(\mathbf{k}) & 0 & 0 \\ 0 & 0 & H_{AB}^{yy}(\mathbf{k}) & 0 \\ 0 & 0 & 0 & H_{AB}^{zz}(\mathbf{k}) \end{pmatrix}$$

where:

$$\begin{aligned} H_{AB}^{00}(\mathbf{k}) &= -\frac{iJ_1}{4} \sum_{\langle iA, jB \rangle} \sum_{\alpha} \langle i b_{iA}^\alpha b_{jB}^\alpha \rangle e^{i\mathbf{k} \cdot \delta_{iA, jB}} \\ H_{AB}^{\alpha\alpha}(\mathbf{k}) &= -\frac{iJ_1}{4} \sum_{\langle iA, jB \rangle} \langle i c_{iA}^\alpha c_{jB}^\alpha \rangle e^{i\mathbf{k} \cdot \delta_{iA, jB}}. \end{aligned} \quad (\text{S6})$$

The self-consistent loop proceeds as follows. A random guess of variational parameters, $\langle i c_{iA}^\alpha c_{jB}^\alpha \rangle, \langle i b_{iA}^\alpha b_{jB}^\alpha \rangle$ is

injected in $H^{MMF}(\mathbf{k})$ and the hamiltonian diagonalized. The set of Lagrange multipliers $\{\lambda_i\}$ is fixed by the single occupancy constraint in Eq. (S2) using a least square minimization. Finally, we find a new set of variational parameters obtained from the mean-field ground state which is a Slater determinant constructed out from the filled orbitals of the mean-field hamiltonian. These three steps are repeated until convergence with the desired tolerance is reached.

We now analyze the π -flux solution to the J_1 - J_2 Heisenberg model discussing the role played by Néel anti-ferromagnetism. We also explore other possible quantum spin disordered solutions such as the valence bond crystal (VBC). We focus on the $0 < J_2/0.5$ regime which is sufficient for our purposes.

A. π -QSL solution

For the π -flux QSL bond pattern shown in Fig. 1 of the main text, the Majorana mean-field hamiltonian is:

$$\begin{aligned} H_{AA}^{00}(\mathbf{k}) &= J_2 \sum_{\alpha} \langle b_{i_A}^{\alpha} i b_{j_A}^{\alpha} \rangle \cos(k_x) \sin(k_y) \\ H_{AA}^{\alpha\alpha}(\mathbf{k}) &= J_2 \langle c_{i_A} i c_{j_A} \rangle \cos(k_x) \sin(k_y), \\ H_{AB}^{00}(\mathbf{k}) &= i \frac{J_1}{4} \sum_{\alpha} \langle b_{i_A}^{\alpha} i b_{j_B}^{\alpha} \rangle (-2i \sin(k_x) + 2 \cos(k_y)) \\ H_{AB}^{\alpha\alpha}(\mathbf{k}) &= i \frac{J_1}{4} \langle c_{i_A} i c_{j_A} \rangle (-2i \sin(k_x) + 2 \cos(k_y)). \end{aligned} \quad (\text{S7})$$

where: $\langle c_{i_A} i c_{j_B} \rangle = \langle b_{i_A}^{\alpha} i b_{j_B}^{\alpha} \rangle > 0$, and $\langle b_{i_A}^{\alpha} i b_{j_A}^{\alpha} \rangle = \langle c_{i_A} i c_{j_A} \rangle < 0$ with $\alpha = x, y, z$ for the flux pattern in Fig. 1 of the main text which has a Chern number of $\nu = -4$. Also we have: $H_{BB}^{00}(\mathbf{k}) = -H_{AA}^{00}(\mathbf{k})$ and $H_{BB}^{\alpha\alpha}(\mathbf{k}) = -H_{AA}^{\alpha\alpha}(\mathbf{k})$.

The resulting Majorana dispersions can be obtained analytically: $\pm 3\gamma(\mathbf{k}), \pm\gamma(\mathbf{k})$ (triply degenerate), with:

$$\gamma(\mathbf{k}) = \frac{J_1}{2} \sqrt{c_1^2 (\sin^2(k_x) + \cos^2(k_y)) + \left(\frac{J_2}{J_1}\right)^2 (2c_2 \cos(k_x) \sin(k_y))^2}, \quad (\text{S8})$$

where: $c_1 = \langle c_{i_A} i c_{j_B} \rangle = \langle b_{i_A}^{\alpha} i b_{j_B}^{\alpha} \rangle$, $c_2 = \langle c_{i_A} i c_{j_A} \rangle = \langle b_{i_A}^{\alpha} i b_{j_A}^{\alpha} \rangle$. These are the expressions quoted in the main text.

The dependence of the π -QSL energy with J_2/J_1 is shown in Fig. S1. The energy is almost constant in the range shown: $E(J_2 = 0) = -0.3442$, $E(J_2 = 0.5) = -0.3443$. The lowering of the energy with J_2 due to the opening of the topological gap is evident, for instance, $E(J_2 = 1) = -0.372675$.

B. π -QSL + Néel antiferromagnetism

An important aspect of the physics of undoped cuprates though, which we have ignored up to now, is Néel antiferromagnetism (AF). For $J_2 = 0$ we expect a Néel state in the square lattice. We have searched for hybrid π -flux QSL + Néel AF solutions. Indeed a non-zero AF moment is present for $0 < J_2 < 0.43$ as shown in Fig. S1. For $J_2 < 0.25$ the Néel-AF is fully saturated, $M = 0, 5$, and so the energy follows the classical linear de-

pendence with J_2 : $E_{Neel} = -0.5 + 0.5J_2$ (taking $J_1 = 1$) shown in Fig. S1. In contrast, for $0.24 < J_2 < 0.43$, a π -QSL+Néel AF *i. e.* a state having $M < 0.5$ and $|\langle c_i c_j \rangle| \neq 0$ arises. A topological transition occurs at $J_2 \sim 0.43$ where Néel antiferromagnetism fades away and the pure π -QSL with $|\nu| = 4$ wins. Fig. S1 indeed shows how the energy of the π -QSL+Néel AF converges to the energy of the pure π -QSL a J_2/J_1 at sufficiently large J_2/J_1 .

Although our MMFT π -QSL + Néel AF is always gapped, the gap for $J_2 < 0.43$ associated with the Néel order is trivial while the gap for $J_2 > 0.43$ in the π -QSL phase is topological with Chern number, $|\nu| = 4$. Hence, even though a hybrid π -flux QSL + Néel AF actually occurs in the MMFT equations, such state is non-topological, in fact only the pure π -QSL is topological. However, this could be an artifact of the MMFT in which broken symmetry states are treated classically.

The hybrid π -QSL + Néel AF state is not the lowest energy state in the whole $0 < J_2/J_1 < 0.5$ range. The spin disordered valence bond crystal (VBC) consisting

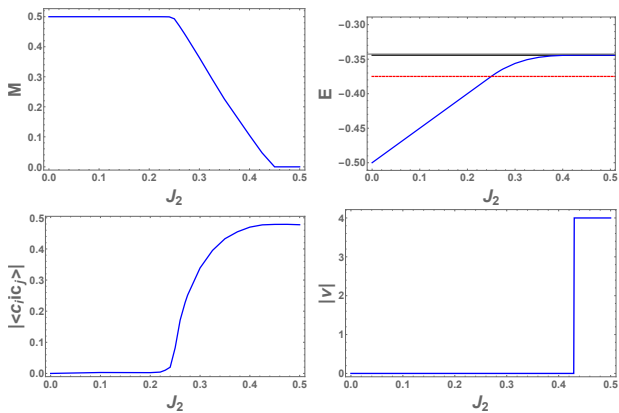


FIG. S1. Dependence of properties of various MMFT solutions with J_2 . From top to bottom: antiferromagnetic moment (M), energy per site (E) absolute value of π -QSL amplitude ($|\langle c_i c_j \rangle|$) and Chern number ($|\nu|$) are shown for the hybrid π -QSL (blue solid lines). The energies of the spin disordered VBC (red solid line) and the pure ($M = 0$) π -QSL (black solid line) are also shown for comparison. $J_1 = 1$ in this plot.

of singlets between n.n. spins, has an energy per site of $E_{VBC} = -0.375$ for any J_2/J_1 since the singlets are effectively decoupled. As shown in Fig. S1 the VBC state wins for $J_2/J_1 > 0.25$, actually the onset of the hybrid π -QSL + Néel AF state occurs. Although our total energy analysis suggests that a direct transition from a Néel AF to a VBC occurs around $J_2 \sim 0.25J_1$, it also indicates that a π -QSL + Néel AF is a possible self-consistent solution of the MMFT. Theories beyond the Majorana mean-field treatment including quantum fluctuations may stabilize a coexistent π -QSL + Néel AF state with non-trivial topological properties.

II. THREE-SPIN MAGNETIC ORBITAL TERM

We now apply the MMFT to the magnetic orbital contribution considered in the main text:

$$H_\phi = J_\phi \sum_{\Delta} \mathbf{S}_i \cdot (\mathbf{S}_j \times \mathbf{S}_k), \quad (\text{S9})$$

where the sum is taken over all triangular placquettes of the square lattice.

This kind of three-spin terms has been discussed in the context of bosonic and fermionic spinon theories of

the Hubbard model in the large- U limit. [2–4] Actually fermionic mean-field theories provide an exact solution of the large- N limit of the model as has been shown in the $SU(N)$ Heisenberg model.[5] In order to make direct contact with these approaches we apply the MMFT decoupling directly onto the large- N expression for the chiral three-spin terms. Our starting point is the full expression of the three-spin contribution expressed in terms of Abrikosov fermions[2]:

$$\mathbf{S}_i \cdot (\mathbf{S}_j \times \mathbf{S}_k) = -\frac{i}{4}(P_{ijk} - P_{ijk}^\dagger) \quad (\text{S10})$$

where $P_{ijk} = (f_{i\alpha}^\dagger f_{i\beta})(f_{j\beta}^\dagger f_{j\gamma})(f_{k\gamma}^\dagger f_{k\alpha})$ exchanges three fermions around the triangular placquette. Note that Einstein notation for the sums over spin indices is assumed here. The mean-field treatment of this contribution consists on contracting only the fermionic operators with the same spin which leads to the large- N expression:

$$\begin{aligned} \mathbf{S}_i \cdot (\mathbf{S}_j \times \mathbf{S}_k) = & -\frac{i}{4}[(f_{j\beta}^\dagger f_{i\beta})(f_{k\gamma}^\dagger f_{j\gamma})(f_{i\alpha}^\dagger f_{k\alpha}) \\ & - (f_{k\alpha}^\dagger f_{i\alpha})(f_{j\gamma}^\dagger f_{k\gamma})(f_{i\beta}^\dagger f_{j\beta})]. \end{aligned} \quad (\text{S11})$$

The fermions satisfy: $\sum_{\alpha} f_{i\alpha}^\dagger f_{i\alpha} = 1$. It can be shown that even for the not so large value $N = 2$ the contractions neglected do not change qualitatively the physics. Defining $\chi_{ij} = f_{j\alpha}^\dagger f_{i\alpha}$ the mean-field hamiltonian, H_ϕ reads:

$$\begin{aligned} H_\phi^{MF} = & i\frac{J_\phi}{4} \sum_{\Delta} [\chi_{ij}\langle\chi_{jk}\rangle\langle\chi_{ki}\rangle - \langle\chi_{ik}\rangle\langle\chi_{kj}\rangle\chi_{ji} \\ & + \langle\chi_{ij}\rangle\chi_{jk}\langle\chi_{ki}\rangle - \langle\chi_{ik}\rangle\chi_{kj}\langle\chi_{ji}\rangle \\ & + \langle\chi_{ij}\rangle\langle\chi_{jk}\rangle\chi_{ki} - \chi_{ik}\langle\chi_{kj}\rangle\langle\chi_{ji}\rangle \\ & - 2(\langle\chi_{ij}\rangle\langle\chi_{jk}\rangle\langle\chi_{ki}\rangle - \langle\chi_{ik}\rangle\langle\chi_{kj}\rangle\langle\chi_{ji}\rangle)], \end{aligned} \quad (\text{S12})$$

where the sum is over all triangular placquettes with vertices ijk .

Performing a Majorana transformation:

$$\begin{aligned} f_{i\uparrow} &= \frac{1}{2}(c_i - ib_i^z), f_{i\uparrow}^\dagger = \frac{1}{2}(c_i + ib_i^z) \\ f_{i\downarrow} &= \frac{1}{2}(b_i^y - ib_i^x), f_{i\downarrow}^\dagger = \frac{1}{2}(b_i^y + ib_i^x), \end{aligned} \quad (\text{S13})$$

leads to the decomposition in terms of the Majoranas:

$$f_{i\alpha}^\dagger f_{j\alpha} = \frac{1}{4}(c_i c_j - ic_i b_j^z + ib_i^z c_j + b_i^z b_j^z + b_i^y b_j^y - ib_i^y b_j^x + ib_i^x b_j^y + b_i^x b_j^x). \quad (\text{S14})$$

We consider mean-field solutions with non-zero bond

fluxes *i.e.* $\langle\chi_{ij}\rangle = \pm iR_{ij}$ with $R_{ij} \in \mathbb{R}$ leading to the terms

$$\langle \chi_{jk} \rangle \langle \chi_{ki} \rangle f_{i\alpha}^\dagger f_{j\alpha} - \langle \chi_{ik} \rangle \langle \chi_{kj} \rangle f_{j\alpha}^\dagger f_{i\alpha} = \pm \frac{1}{4} R_{jk} R_{ki} \times [(c_i c_j - c_j c_i) + (b_i^x b_j^x - b_j^x b_i^x) + (b_i^y b_j^y - b_j^y b_i^y) + (b_i^z b_j^z - b_j^z b_i^z)]. \quad (\text{S15})$$

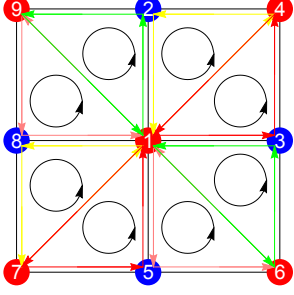


FIG. S2. Three-spin magnetic orbital interactions.

where the final overall sign in front depends on the final bond flux orientation. Hence, the final hamiltonian, H_ϕ^{MF} , will only contain diagonal contributions. Since H_ϕ^{MF} as well as the Heisenberg hamiltonian is diagonal in the Majoranas, we have that:

$$R_{ij} = \frac{1}{4} (\langle c_i c_j \rangle + \sum_{\alpha} \langle b_i^{\alpha} b_j^{\alpha} \rangle). \quad (\text{S16})$$

$$\mathbf{S}_1 \cdot (\mathbf{S}_3 \times \mathbf{S}_2 + \mathbf{S}_3 \times \mathbf{S}_4 + \mathbf{S}_6 \times \mathbf{S}_3 + \mathbf{S}_5 \times \mathbf{S}_3 + \mathbf{S}_2 \times \mathbf{S}_8 + \mathbf{S}_9 \times \mathbf{S}_8 + \mathbf{S}_8 \times \mathbf{S}_7 + \mathbf{S}_8 \times \mathbf{S}_5)$$

are involved in the 1 – 4 and 1 – 7 n.n.n. couplings, the terms:

$$\mathbf{S}_1 \cdot (\mathbf{S}_6 \times \mathbf{S}_3 + \mathbf{S}_5 \times \mathbf{S}_6 + \mathbf{S}_2 \times \mathbf{S}_9 + \mathbf{S}_9 \times \mathbf{S}_8) \quad (\text{S18})$$

renormalize the n.n. 1 – 3 and 1 – 8 couplings while:

$$\mathbf{S}_1 \cdot (\mathbf{S}_2 \times \mathbf{S}_9 + \mathbf{S}_2 \times \mathbf{S}_8 + \mathbf{S}_4 \times \mathbf{S}_2 + \mathbf{S}_3 \times \mathbf{S}_2 + \mathbf{S}_5 \times \mathbf{S}_6 + \mathbf{S}_5 \times \mathbf{S}_3 + \mathbf{S}_7 \times \mathbf{S}_5 + \mathbf{S}_8 \times \mathbf{S}_5), \quad (\text{S19})$$

the n.n. 1 – 2 and 1 – 5 couplings.

The three-spin terms evaluated on zero-flux mean-field solutions such as a zero-flux QSL or a VBC solution leads to cancellations so that $\langle H_\chi^{MF} \rangle = 0$. Hence, to illustrate

the effect of the three-spin terms we evaluate H_χ^{MF} on a π -QSL bond pattern. Introducing the corresponding MMFT bond amplitudes $\langle c_i c_j \rangle$ and $\langle b_i^{\alpha} b_j^{\alpha} \rangle$ in R_{ij} we find the complete mean-field hamiltonian (including the Heisenberg contribution):

$$\begin{aligned} H_{AA}^{00}(\mathbf{k}) &= (J_2 \sum_{\alpha} \langle b_{iA}^{\alpha} i b_{jA}^{\alpha} \rangle + J_{\phi} R_1^2) \cos(k_x) \sin(k_y) \\ H_{AA}^{\alpha\alpha}(\mathbf{k}) &= (J_2 \langle c_{iA} i c_{jA} \rangle + J_{\phi} R_1^2) \cos(k_x) \sin(k_y), \\ H_{AB}^{00}(\mathbf{k}) &= \frac{i}{4} (J_1 \sum_{\alpha} \langle b_{iA}^{\alpha} i b_{jB}^{\alpha} \rangle + J_{\phi} R_1 R_2) (-2i \sin(k_x) + 2 \cos(k_y)) \\ H_{AB}^{\alpha\alpha}(\mathbf{k}) &= \frac{i}{4} (J_1 \langle c_{iA} i c_{jA} \rangle + J_{\phi} R_1 R_2) (-2i \sin(k_x) + 2 \cos(k_y)), \end{aligned} \quad (\text{S20})$$

where $R_{ij} = R_1$ for nearest-neighbor and $R_{ij} = R_2$ for

next-nearest-neighbor bonds. We also have: $H_{BB}^{00}(\mathbf{k}) =$

$-H_{AA}^{00}(\mathbf{k})$ and $H_{BB}^{\alpha\alpha}(\mathbf{k}) = -H_{AA}^{\alpha\alpha}(\mathbf{k})$. From the mean-field hamiltonian derived in Eq. (S20) it is evident that the three-spin terms just modify the bare Heisenberg amplitudes of the π -QSL solution. It is worth noting that even a pure H_ϕ model with infinitesimally small non-zero J_ϕ will induce a π -QSL on the square lattice.

III. MAGNETIC ORDER FROM EXACT DIAGONALIZATION

The various magnetic orders in the models considered are investigated by evaluating the ED static spin structure factor:

$$S(\mathbf{Q}) = \frac{1}{N} \sum_{ij} e^{i\mathbf{Q}\cdot(\mathbf{R}_i - \mathbf{R}_j)} \langle \mathbf{S}_i \cdot \mathbf{S}_j \rangle, \quad (\text{S21})$$

where N is the number of sites of the cluster.

In Fig. S3 we compare the $S(\mathbf{Q})$ calculated on a 4×4 cluster for different parameters of the $J_1 - J_2 - D$ and $J_1 - J_2 - J_\phi$ models. The Néel and collinear phases display a large clear structure at their corresponding (π, π) and $(\pi, 0)$ ordering wavevectors, respectively. This behavior is in contrast to the structureless $S(\mathbf{Q})$ of the possible spin disordered phase (around $J_2/J_1 = 0.6$) or the weak structure around $(\pi, 0)$ ($(\pi, \pi/2)$) of the J_ϕ (D) dominated phase. The fact that these three last phases display comparable value of $S(\mathbf{Q})$ indicate that they are disordered or very weakly magnetically ordered.

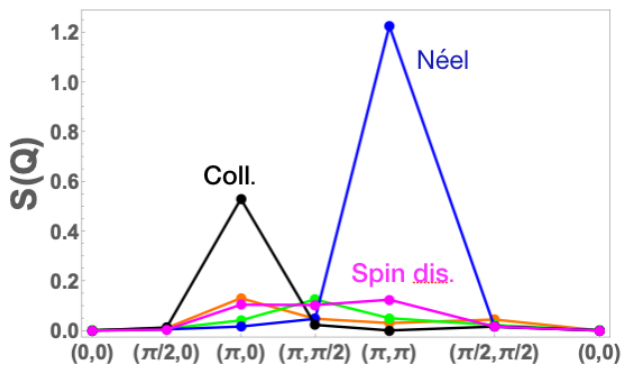


FIG. S3. Effect of J_ϕ and D on magnetic order of the Heisenberg model on the square lattice. The spin structure factor, $S(\mathbf{Q})$, obtained from exact diagonalization on a 4×4 cluster is shown along the path in the first Brillouin zone of Fig. 1 of the main text. We compare the $S(\mathbf{Q})$ in the Néel, $J_2/J_1 = 0$, $J_\phi = D = 0$ (blue line) collinear, $J_2/J_1 = 1$, $J_\phi = D = 0$ (black line), spin disordered, $J_2/J_1 = 0.6$, $J_\phi = D = 0$ (pink line), $J_2/J_1 = 0.6$, $J_\phi = 1$, $D = 0$ (orange line) and D -state $J_2/J_1 = 0.6$, $D = 1$ (green line). $S(\mathbf{Q})$ is only evaluated at the points shown so the lines are just guides for the eye.

IV. DZYLASHINSKII-MORIYA CONTRIBUTION

In this section, we discuss the phase diagram of the $J_1 - J_2 - D$ model in the presence of a spin-orbit coupling that forces the spin rotations to be coupled with real-space symmetry transformations. The Dzyaloshinskii-Moriya (DM) term is defined as:

$$H_{\text{DM}} = \sum_{\langle i,j \rangle} \vec{D}_{ij} \cdot (\vec{S}_i \times \vec{S}_j) \quad (\text{S22})$$

where \vec{D}_{ij} are the DM vectors. As said in the paper, we have considered five compatible DM vector choices, YBCO, LSCO-LTO, LSCO-LTT for the ones compatible with cuprates, and the ones expected to realize Rashba-like and Dresselhaus-like SO as observed for electronic systems, considered by [6]. The corresponding \vec{d}_i vectors as displayed in Fig. 1 of the paper are defined as: (i) YBCO with $\vec{d}_1 = \vec{d}_3 = (d, 0, 0)$ and $\vec{d}_2 = \vec{d}_4 = (0, -d, 0)$, (ii) LSCO-LTO with $\vec{d}_1 = -\vec{d}_3 = (d, 0, 0)$ and $\vec{d}_2 = -\vec{d}_4 = (0, -d, 0)$, (iii) LSCO-LTT with $\vec{d}_1 = -\vec{d}_3 = (0, d, 0)$ and $\vec{d}_2 = -\vec{d}_4 = (0, d, 0)$, (iv) Rashba with $\vec{d}_1 = \vec{d}_3 = (0, d, 0)$ and $\vec{d}_2 = \vec{d}_4 = (-d, 0, 0)$ and (v) Dresselhaus with $\vec{d}_1 = \vec{d}_3 = (0, -d, 0)$ and $\vec{d}_2 = \vec{d}_4 = (-d, 0, 0)$.

The effect of the DM term can be considered by employing the MMFT. Since the DM term only contains two spin operators, using Eq. S3 it is straightforward to mean field decouple the following terms:

$$\begin{aligned} D^x (S_i^y S_j^z - S_i^z S_j^y), \\ D^y (S_i^z S_j^x - S_i^x S_j^z), \\ D^z (S_i^x S_j^y - S_i^y S_j^x). \end{aligned}$$

For each case, we have systematically compared the energies of the 2 most relevant ansätze in the MMFT, namely the VBC state and the π -QSL state. This is displayed in Fig. S4.

Three important features can be noted. First, the π -QSL is always a stable ansatz of our MMFT. Second, the VBC is always lower in energy than the π -QSL, whatever the choice of the DM vectors. Finally, the π -QSL is also always lowered w.r.t. D indicating that the effect of SO coupling is positive, in the sense that it continues to favor it even though it is an excited state.

To further understand the role of the DM term, we have solved the $J_1 - J_2 - D$ Hamiltonian by using exact diagonalizations on a 16 site cluster and the Majorana mean field theory for the case compatible with YBCO compounds. In Fig. S6, we show a ternary plot with the constraint $J_1 + J_2 + D = 1$, of the first gap obtained by ED. We immediately see five distinct domains separated by zero gap lines (white regions). Along the $D = 0$ line, we recover the Néel region (close to $J_1 = 1$), the intermediate disordered phase ($0.4 < J_2 < 0.6$) and

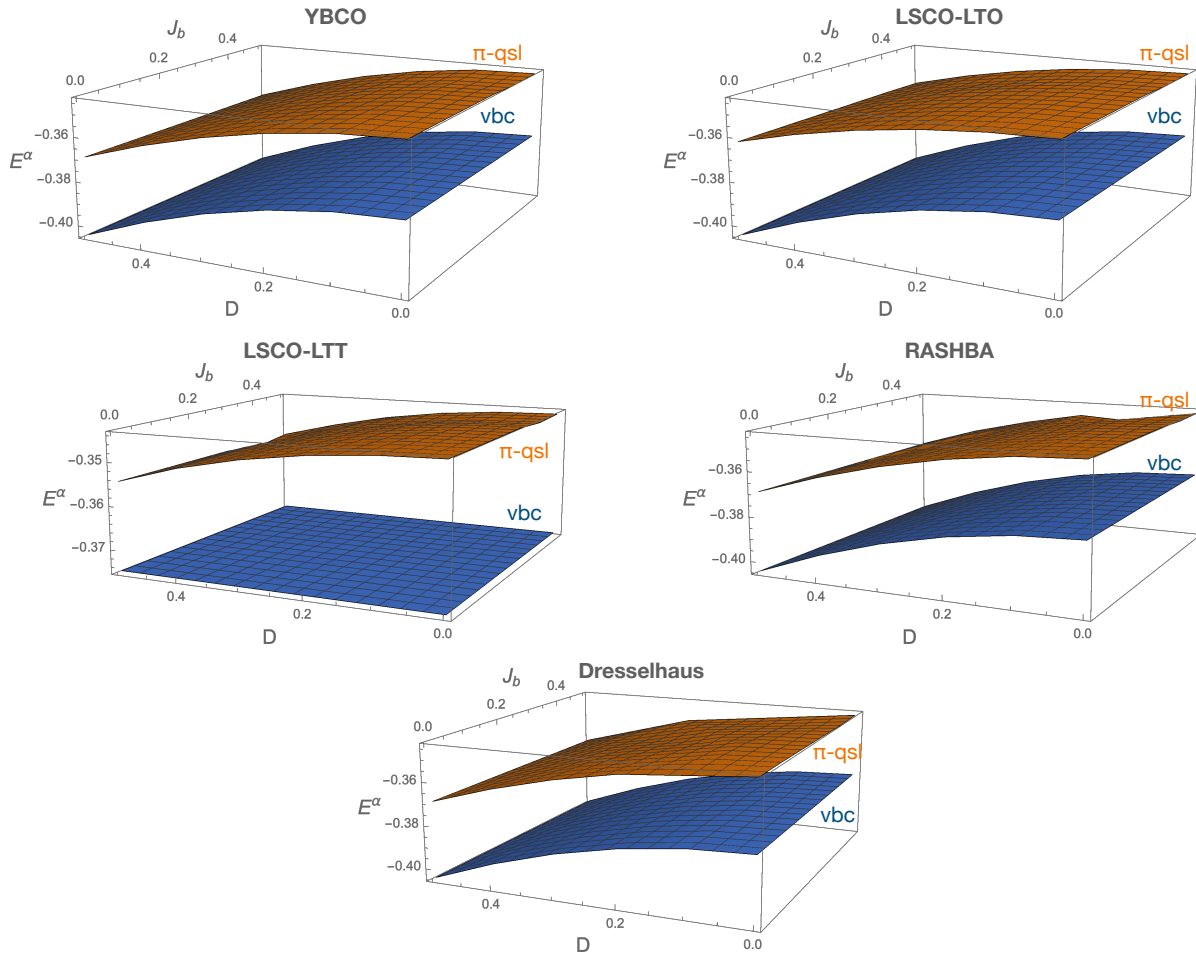


FIG. S4. Comparison of the energy of the VBC and the π -QSL ansätze for the five compatible DM vector choices. The π -QSL remains always an excited state w.r.t. to VBC one, but the effect of D is to lower its energy hence indicating a positive effect of SO coupling onto this state.

the collinear phase at higher J_2 . In order to characterize these phases we have calculated the quantum fidelity $|\langle \psi_{\text{ref}} | \psi_0 \rangle|$ in the whole parameter space by starting from 4 reference states $|\psi_{\text{ref}}\rangle$ chosen deep in their corresponding expected parameter regions. They are indicated by black points in Fig.S5 for each of the 4 panels, and the value of the quantum fidelity, ranging from 0 to 1, scales from white (0) to full colored (1) hexagons respectively.

Strikingly, already on such a limited cluster, the fidelity gives strong indications about the phase boundary locations. For instance, from the overlap with the pure Néel state obtained at $J_1 = 1$, we find that the Néel region extends in the lower right part of the ternary plot (yellow points). A very small, yet finite, fidelity can be found in the DM region as J_1 decreases, but considering that the Néel region is unambiguously characterized by a fidelity close to one then, along the $J_2 = 0$ line, the Néel region ends around $J_1 \simeq 0.4$. What is remarkable here is that the Néel, the DM and the collinear regions are well

separated even when the transition is second order (no level crossings).

As previously mentioned, starting from a different reference state allows us to span entire regions of this model with close-to-one fidelities. This is in particular the case for the intermediate region (blue centered domain of the upper-left panel of Fig. S5) delimited by a frontier of zero energy gap as can be observed in Fig.S6. This region (the blue one in Fig.S5) is gapped and possibly magnetically disordered since the spin structure factor, $S(\mathbf{Q})$, is rather featureless displaying only weak structures as shown in Fig. S3. We have denoted this intermediate phase the DM state in the main text. Finally, at large D , the system enters a fourth phase which is magnetically ordered. This can be interpreted as a quantum version of the magnetic DM state obtained with the MMFT approach. To the best of our knowledge, such intermediate possibly disordered DM state has never been reported so far.

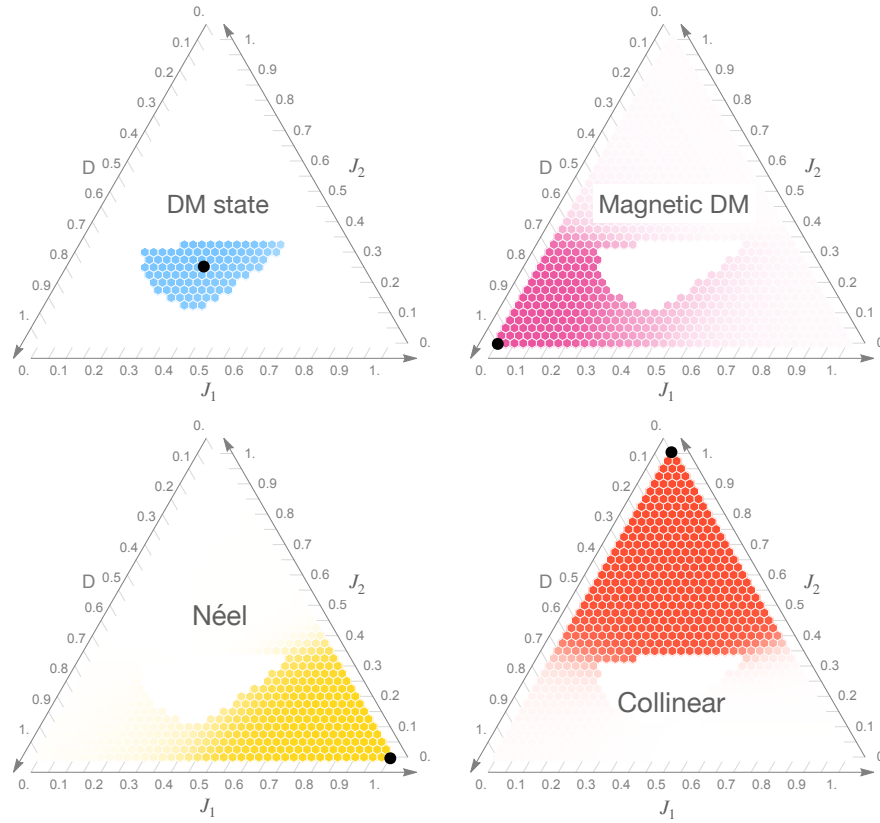


FIG. S5. Quantum fidelity computed by ED for 4 different reference sites (black points). A quantum fidelity of 1 corresponds to full colored point while a zero one corresponds to white hexagons. Four clear regions can be clearly identified, as mentioned in Fig. S6. The disordered phase of the raw $J_1 - J_2$ model cannot be clearly identified in such a small cluster, but clearly appears in the gap of Fig. S6 (extended white region).

V. DETAILS ON THE TEMPERATURE DEPENDENCE OF THERMAL HALL CONDUCTIVITY

In the main text we have stated that the thermal Hall conductivity can be fitted in a broad temperature range to an exponential form $\kappa_{xy}/T \propto e^{-T/T_0}$. Such exponential forms are observed experimentally in an intermediate temperature range [7]. Here we provide details about these fits. Our theoretical calculations can be nicely fitted to the following expressions: $\kappa_{xy}/T \sim A + Be^{-T/T_0}$ as shown in Fig. S7. For $J_2/J_1 = 1/3$ the fit is: $\kappa_{xy}/T \sim -0.02508 - 1.02225e^{-T/0.015}$, for $J_2/J_1 = 0.5$ the fit is: $\kappa_{xy}/T \sim -0.0905446 - 1.13263e^{-T/0.029}$ and for $J_2/J_1 = 1$ the fit is: $\kappa_{xy}/T \sim -0.0821182 - 1.41715e^{-T/0.08045}$. Using appropriate parameters for

the cuprates $J_1 \sim 0.1\text{eV}$ would lead to the temperature scales: $T_0(J_2/J_1 = 1/3) \sim 18\text{K}$, $T_0(J_2/J_1 = 1/2) \sim 35\text{K}$ and $T_0(J_2/J_1 = 1) \sim 93.4\text{K}$.

We can compare our theoretical MMFT results with the 2D thermal conductivity obtained from experiments. Experimental data of La_2CuO_4 and $\text{Sr}_2\text{CuO}_2\text{Cl}_2$ has been found to have the T -dependence: $\kappa_{xy}^{expt}/T \sim (-0.0132 - 3.234e^{-T/T_0^{expt}}) \times 10^{-9} \frac{\text{mW}}{\text{K}^2}$ with $T_0^{expt} \sim 17\text{K}$. The theoretical curve with closest T_0 corresponds (taking $J_1 \sim 0.1\text{eV}$) to $J_2/J_1 = 1/3$ ($T_0 \sim 18\text{K}$) and has the T -dependence: $\kappa_{xy}/T \sim (-0.01618 - 1.2073e^{-T/T_0}) \times 10^{-9} \frac{\text{mW}}{\text{K}^2}$. Since the cuprates are typically in the low J_2/J_1 parameter regime, we conclude that our MMFT predictions for κ_{xy} are consistent with available experimental data.

- [1] A. Kitaev, Anyons in an exactly solvable model and beyond, *Ann. Phys. (Amsterdam)* **321**, 2 (2006).
 [2] O. I. Motrunich, Orbital magnetic field effects in spin liquid with spinon Fermi sea: possible application to κ -(ET) $_2\text{Cu}_2(\text{CN})_3$, *Phys. Rev. B* **73**, 155115 (2006).

- [3] J. H. Han, J.-H. Park, and P. A. Lee, Consideration of thermal Hall effect in undoped cuprates, *Phys. Rev. B* **99**, 205157 (2019).
 [4] R. Samajdar, S. Chatterjee, S. Sachdev, and M. S. Scheurer, Thermal Hall effect in square-lattice spin liq-

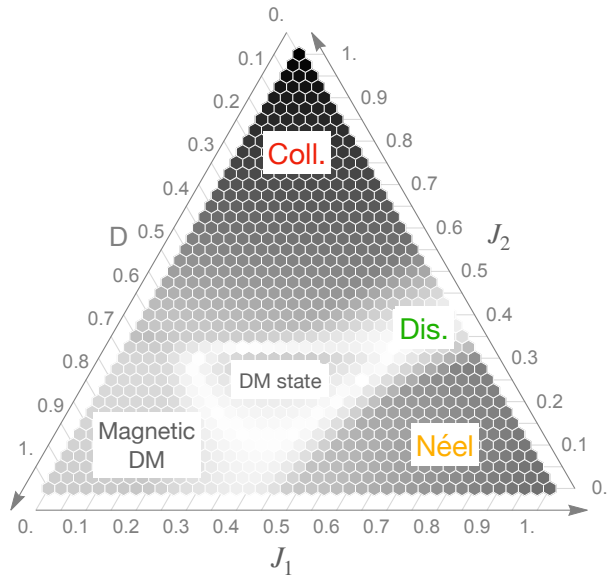


FIG. S6. Density map of the gap ΔE on a ternary plot satisfying $J_1 + J_2 + D = 1$ obtained by ED on the 16-site cluster. The more white the density, the smaller the gap. Five phases are observed, the Néel, the disordered and the collinear phases from the original $J_1 - J_2$ model that largely extend in the phase diagram, an ordered phase driven by D called magnetic DM and a trivial and possibly disordered intermediate phase dubbed DM state, delimited by frontiers of zero gap (white lines).

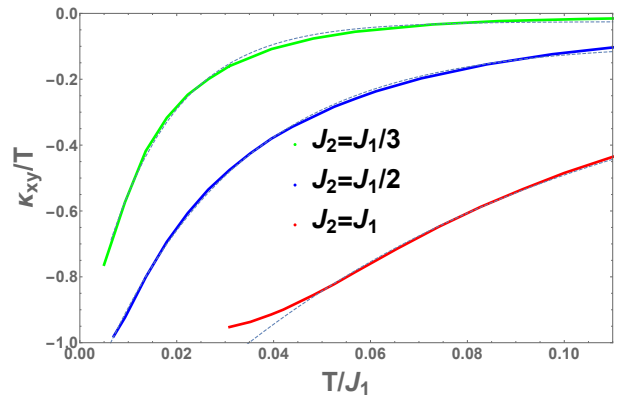


FIG. S7. Exponential temperature dependence of the thermal Hall conductivity. Fits of our calculated MMFT thermal Hall conductivity to: $\kappa_{xy}/T \sim A + Be^{-T/T_0}$ are shown.

uids: A Schwinger boson mean-field study, Phys. Rev. B **99**, 165126 (2019).

- [5] Assa Auerbach, *Interacting electrons and quantum magnetism*, Springer (1994).
- [6] M. Kawano, Y. Onose and C. Hotta, Designing Rashba-Drusselhaus effect in magnetic insulators, Comm. Phys. **2**:27 (2019)
- [7] G. Grissonnanche, *et. al.*, Chiral phonons in the pseudogap phase of cuprates, Nat. Phys. **16** 1108 (2020).